see commentary on page 1125

Accumulation of advanced oxidation protein products induces podocyte apoptosis and deletion through NADPH-dependent mechanisms

Li Li Zhou[1], Fan Fan Hou[1], Guo Bao Wang[1], Fang Yang[1], Di Xie[1], Yong Ping Wang[1] and Jian Wei Tian[1]

[1]*Division of Nephrology, Nanfang Hospital, Southern Medical University and Key Lab for Organ Failure Research, Ministry of Education, Guangzhou, P.R. China*

The accumulation of plasma advanced oxidation protein products (AOPPs) is prevalent in diverse disorders such as diabetes, metabolic syndromes, and chronic kidney disease. To study whether accumulated AOPPs have an important role in the progression of proteinuria and glomerulosclerosis, we chronically treated normal Sprague–Dawley rats with AOPP-modified rat serum albumin. Podocyte apoptosis was significantly increased coincident with the onset of albuminuria and preceded significant losses of glomerular podocytes. Increasing the amount of AOPPs in the media of conditionally immortalized podocytes rapidly triggered the production of intracellular superoxide by activation of NADPH oxidase and this, in turn, led to an upregulation of p53, Bax, caspase 3 activity, and apoptosis. Chronic inhibition of NADPH oxidase by apocynin prevented podocyte apoptosis, ameliorated podocyte depletion, and decreased albuminuria in AOPP-challenged rats. Our study demonstrates that accumulation of AOPPs promotes NADPH oxidase–dependent podocyte depletion by a p53-Bax apoptotic pathway both *in vivo* and *in vitro*.

Kidney International (2009) **76,** 1148–1160; doi:10.1038/ki.2009.322; published online 2 September 2009

KEYWORDS: AOPPs; NADPH oxidase; podocyte apoptosis; podocyte depletion

Correspondence: *Fan Fan Hou, Division of Nephrology, Nanfang Hospital, Southern Medical University, 1838 North Guangzhou Avenue, Guangzhou 510515, P.R. China. E-mail: ffhou@public.guangzhou.gd.cn*

Received 26 February 2009; revised 14 June 2009; accepted 7 July 2009; published online 2 September 2009

Progression to renal parenchymal damage and end-stage renal disease, which seems to be largely independent of the initial insults, is the common pathway for chronic kidney disease (CKD) in both animals and humans.[1,2] The key event of the pathway is the impairment of glomerular permeability to proteins, which permits excessive amounts of proteins to reach the lumen of the proximal tubule and contributes to renal interstitial injury by activating inflammatory and fibrogenic cascades.[3,4]

Glomerular visceral epithelial cell, or podocyte, is one of the major cell types in the glomerulus. The podocyte forms a critical part of the glomerular filtration barrier and functions to prevent urinary protein leakage and to maintain glomerular capillary loop integrity.[5] Podocyte depletion leads to areas of denuded glomerular basement membrane, culminating in proteinuria and development of glomerulosclerosis.[6] There is a growing body of literature showing that podocyte loss is related to increasing proteinuria and contributes to the progression of kidney disease in both diabetic and nondiabetic CKD.[7–13]

Numerous factors have been implicated in the pathogenesis of podocyte injury and depletion: hyperglycemia, angiotensin II, reactive oxygen species, and transforming growth factor-β have been extensively characterized.[14–18] Recently, a family of oxidized protein compounds, termed 'advanced oxidation protein products' (AOPPs), has emerged as a novel class of renal pathogenic mediators. AOPPs are a class of dityrosine-containing protein products formed during oxidative stress and carried mainly by albumin *in vivo*.[19,20] Accumulation of plasma AOPPs was first identified in patients who underwent dialysis [19] and was subsequently found in subjects with diabetes,[21,22] metabolic syndrome,[23] and nondiabetic CKD.[20] Our recent studies have shown that chronic accumulation of plasma AOPPs significantly increases urinary protein excretion and accelerates glomerulosclerosis in a remnant kidney model.[24] An increase in the concentration of plasma AOPPs to the level that has been found in diabetic patients increases urinary excretion of albumin in both normal and streptozotocin-induced diabetic rats.[24,25] Consistent with these observations, data from a clinical study have shown that plasma AOPP level

is a strong predictor for the prognosis of IgA nephropathy.[26] Although these observations suggest that AOPP accumulation has an important role in the progression of proteinuria and glomerulosclerosis, the underlying cellular and molecular mechanism(s) have not been clarified. It remains unknown whether AOPPs affect structure and function of the podocyte.

Two underlying mechanisms for podocyte loss are apoptosis and detachment. Apoptosis in glomerular cells has been demonstrated in animal models as well as in patients with chronic renal insufficiency, diabetes, and hypertension nephrosclerosis,[27–30] in which the accumulation of AOPPs is implicated. Therefore, this study was designed to determine the contribution of AOPPs to podocyte loss. Our data show that the accumulation of AOPPs results in podocyte loss through the induction of apoptosis. AOPP-induced podocyte apoptosis is mainly mediated by the nicotinamide adenine dinucleotide phosphate (NADPH) oxidase-dependent superoxide generation, which activates the p53–Bcl-2-associated X (Bax)–caspase-3 proapoptotic pathway.

RESULTS

Chronic administration of AOPPs increased urinary albumin and 8-hydroxydeoxyguanosine excretion

To examine the renal pathogenic effects of AOPPs *in vivo*, normal Sprague–Dawley rats were randomly assigned to four groups and were treated with intravenous injection of AOPP-modified rat serum albumin (RSA) in the presence or absence of the NADPH oxidase inhibitor apocynin for 5–12 weeks. Plasma AOPP levels increased approximately onefold in AOPP-RSA-treated rats compared with that in vehicle- or RSA-treated controls (Table 1). Chronic administration of AOPP-RSA, but not that of native RSA, significantly enhanced the renal deposition of AOPPs, increased urinary albumin excretion, and elevated the level of urinary 8-OHdG (8-hydroxydeoxyguanosine), a well-known biomarker of oxidative stress *in vivo*.[1] Intervention of apocynin significantly attenuated albuminuria and decreased urinary 8-OHdG level in AOPP-challenged rats. There was no significant difference in serum creatinine levels among the groups (Table 1).

Table 1 | Metabolic and biochemical parameters of rats at week 5 and week 12

Parameters	Week 5[a] (n = 10)	Week 12[a] (n = 10)
Body weight (g)		
Vehicle	329.24 ± 24.29	396.07 ± 17.50
RSA	325.33 ± 26.06	396.21 ± 13.58
AOPPs	306.60 ± 26.64	388.11 ± 33.42
AOPPs+apocynin	315.89 ± 24.44	390.27 ± 28.99
Systolic blood pressure (mm Hg)		
Vehicle	118.28 ± 3.47	123.56 ± 3.18
RSA	120.33 ± 4.16	126.45 ± 3.59
AOPPs	121.25 ± 3.79	125.97 ± 4.03
AOPPs+apocynin	120.40 ± 3.75	122.49 ± 4.15
Urinary albumin excretion (μg per 24 h)[b]		
Vehicle	152.95 ± 84.11	163.63 ± 116.63
RSA	205.28 ± 139.35	243.32 ± 130.24
AOPPs	759.69 ± 125.38[c]	1548.90 ± 324.16[c]
AOPPs+apocynin	203.52 ± 49.93[d]	273.86 ± 90.26[d]
Urinary 8-OHdG excretion (ng per 24 h)[e]		
Vehicle	475.10 ± 178.97	454.86 ± 185.47
RSA	445.04 ± 223.72	488.15 ± 313.82
AOPPs	1346.31 ± 263.56[c]	2279.34 ± 430.46[c]
AOPPs+apocynin	827.29 ± 235.82[c,d]	1076.07 ± 520.22[c,d]
Serum creatinine (μmol/l)[f]		
Vehicle	35.1 ± 2.1	35.3 ± 3.1
RSA	34.7 ± 4.0	34.3 ± 3.3
AOPPs	35.3 ± 2.6	35.2 ± 4.2
AOPPs+apocynin	35.5 ± 3.3	35.7 ± 2.7
Plasma AOPPs (μmol/l)[g]		
Vehicle	27.72 ± 3.51	27.90 ± 4.31
RSA	26.94 ± 6.83	28.93 ± 7.75
AOPPs	60.92 ± 14.67[c]	76.87 ± 18.73[c]
AOPPs+apocynin	43.19 ± 10.66[c,d]	58.86 ± 10.36[c,d]
AOPP level in renal tissue (μmol/g protein)[g]		
Vehicle	8.03 ± 1.43	8.16 ± 2.94
RSA	8.11 ± 2.31	9.94 ± 3.62
AOPPs	19.35 ± 3.93[c]	25.33 ± 6.23[c]
AOPPs+apocynin	15.65 ± 5.22[c,d]	18.95 ± 7.68[c,d]

ANOVA, analysis of variance; AOPP, advanced oxidation protein product; 8-OHdG, 8-hydroxydeoxyguanosine; ELISA, enzyme-linked immunosorbent assay; RSA, rat serum albumin.
[a]Data are mean ± s.d.
[b]Urinary albumin excretion was measured using an ELISA kit, ANOVA, $P<0.001$.
[c]$P<0.05$ vs vehicle.
[d]$P<0.05$ vs AOPPs.
[e]Urinary 8-OHdG level was analyzed using a commercial kit, ANOVA, $P<0.001$.
[f]Serum creatinine was measured by enzymatic assay (CRE-EN, Kynos, Tokyo, Japan).
[g]AOPP levels in the plasma and in renal tissue were measured as described in Li *et al.*[24], ANOVA, $P<0.001$.

Podocyte apoptosis increased in AOPP-challenged rats and was ameliorated by treatment with apocynin

To determine whether AOPP accumulation induces podocyte apoptosis and to delineate the relationship between apoptosis and changes in podocyte number, we first quantified rates of podocyte apoptosis using double-immunofluorescence labeling, including Wilms's tumor-1 and terminal deoxyuridine nick-end labeling (TUNEL) assay. TUNEL-positive podocytes per glomerular cross-section were significantly increased in AOPP-treated rats from week 5 compared with age-matched control animals (vehicle- or RSA-treated rats) (Figure 1a and b). Interestingly, apoptosis was also detectable in tubular epithelial cells, particularly in AOPP-treated rats (data not shown). Treatment of apocynin significantly prevented podocytes from AOPP-induced apoptosis (Figure 1a and b), indicating that the apoptotic processes are dependent on the activation of NADPH oxidase.

To further confirm the *in vivo* proapoptotic effect of AOPPs on podocytes, we next identified and quantified podocytes in urine sediments. Podocytes in cytospin urine sediments were identified as either nucleated or multinucleated cells expressing podocalyxin, using an immunofluorescence microscope. As shown in Figure 1c, no urinary podocytes were detected in rats treated with vehicle or native RSA. The mean value of podocytes per milliliter urine among

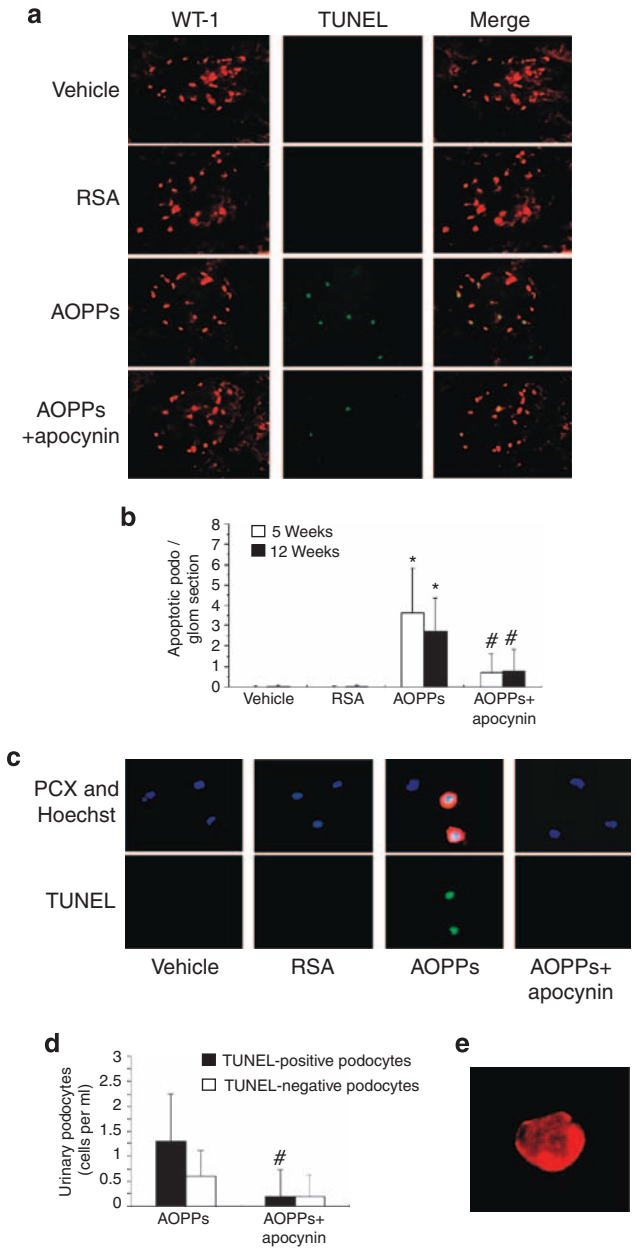

Figure 1 | Accumulation of AOPPs induced podocyte apoptosis and podocyturia. Podocyte apoptosis in the glomeruli: (**a**) Representative photographs showing double-immunofluorescence labeling of WT-1 (red) and TUNEL (green) in podocytes in the glomeruli from rats treated with or without AOPP-RSA. (**b**) Bar graphs show the mean number of WT-1 and TUNEL-positive podocytes per glomerular cross-section. Apoptotic podocytes in urine: (**c**). Representative photographs of triple-fluorescence labeling of urine sediments using Hoechst nuclear staining (blue), goat anti-rat podocalyxin (PCX) IgG (red), and TUNEL (green). (**d**) The mean number of podocytes (PCX-positive cells) and apoptotic podocytes (PCX and TUNEL-positive cells) in urine at week 5. (**e**) Representative double-nuclei podocyte in urine. Data are shown as mean ± s.d., $n = 10$ in each group. $^{*}P < 0.01$ vs vehicle; $^{\#}P < 0.01$ vs AOPPs. AOPP, advanced oxidation protein product; IgG, immunoglobulin G; RSA, rat serum albumin; TUNEL, terminal deoxyuridine nick-end labeling; WT-1, Wilms's tumor-1.

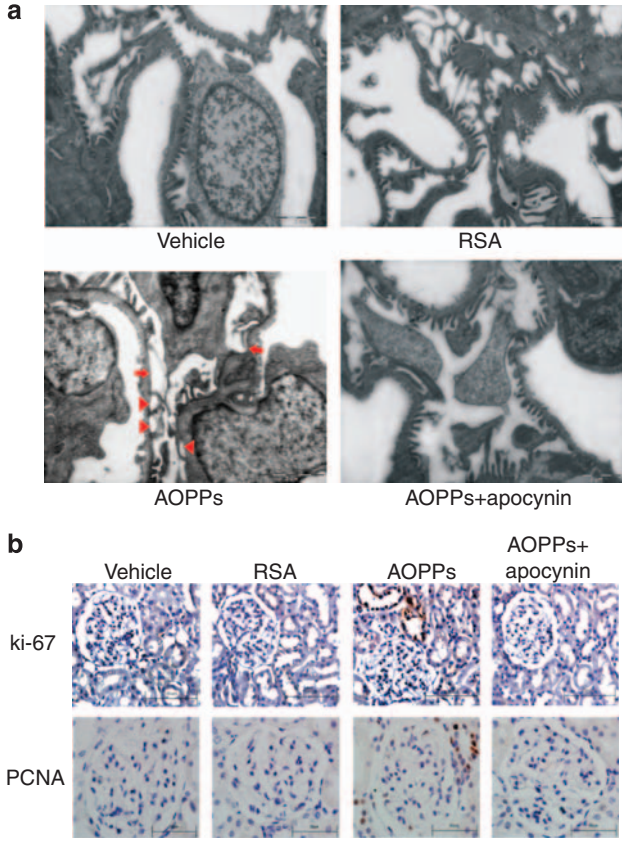

Figure 2 | Morphological changes and immunohistochemical staining of ki-67 and PCNA. (**a**) Representative electron-micrographs of rats treated with or without AOPP-RSA (original magnification: ×15,000). Loss or flattening of foot processes, local detachments leaving behind naked areas of GBM (arrowheads), and denudation of GBM (arrows) were found in AOPP-treated rats; these could be largely prevented by apocynin treatment. (**b**) Immunohistochemical analysis showed that expression of ki-67 (bar = 100 μm) and PCNA (bar = 50 μm) was located mainly in tubular epithelial cells. AOPP, advanced oxidation protein product; GBM, glomerular basement membrane; PCNA, proliferating cell nuclear antigen; RSA, rat serum albumin.

the animals treated with AOPP-RSA was 1.90 ± 1.14 ($n = 10$) at week 5, with 68% of podocytes being apoptotic (indicated by positive TUNEL staining). Podocyturia in AOPP-treated rats appeared from week 3 and attained peak level at week 5 (data not shown). Intervention of apocynin significantly decreased podocyturia and urinary apoptotic podocytes at week 5 (Figure 1c–e).

Podocyte loss occurred in AOPP-challenged rats and was blocked by treatment with apocynin

To examine whether AOPP-induced podocyte apoptosis results in glomerular podocyte loss, we first examined the morphological changes in podocytes under electron microscopy. As shown in Figure 2, specific indicators of podocyte injury,[31] including flattening of foot processes, local detachments of foot processes with loss of podocytes, leaving areas of denuded glomerular basement membrane, and loss of

entire podocytes were found in AOPP-treated rats, which was largely ameliorated by treatment with apocynin (Figure 2). Similarly, podocyte number and podocyte density, as analyzed using stereological methods, were significantly reduced in AOPP-treated rats at week 12 compared with controls. Treatment of apocynin significantly ameliorated the AOPP-induced podocyte loss in the glomeruli (Table 2).

To determine whether podocyte apoptosis is associated with cellular regeneration, we examined the expression of ki-67 and proliferating cell nuclear antigen (PCNA) in kidney sections. Expression of ki-67 and PCNA was mainly located in tubular epithelial cells in AOPP-treated animals (Figure 2).

Increase in extracellular AOPPs was sufficient to trigger apoptosis of podocytes *in vitro* by NADPH-dependent superoxide generation

To further confirm the proapoptotic effect of AOPPs on the podocyte, cultured murine podocytes were incubated with indicated concentration of AOPP-modified murine serum albumin (MSA) for 48 h or treated with 200 μg/ml of AOPP-MSA for the indicated time. Exposure of podocytes to AOPP-MSA induced dose- and time-dependent increase in apoptosis as assessed by Annexin V (AV)-labeled cells. AOPP fraction isolated from patients with uremia showed a similar effect on cultured podocytes (Figure 3a). Increased apoptosis in podocytes incubated with AOPP-MSA was also shown by analysis of DNA strand breaks with the TUNEL assay (Figure 3b) and electron microscopic analysis (Figure 3c). AOPP-induced apoptosis could be largely blocked by treatment of apocynin (Figure 3b and c).

To clarify the underlying mechanism of AOPP-induced podocyte apoptosis, podocytes were preincubated for 1 h with the inhibitors of various enzymatic systems involved in reactive oxygen species generation, a broad spectrum inhibitor of protein kinase C (PKC) (Gö6983), and an intracellular superoxide (O_2^-) scavenger (cytosolic Cu/Zn superoxide dismutase, c-SOD), respectively. The cells were then incubated with AOPP-MSA for 48 h. AOPP-MSA-induced podocyte apoptosis was significantly suppressed by the NADPH oxidase inhibitors, DPI (diphenyleneiodonium) and apocynin, the PKC inhibitor, Gö6983, and c-SOD, but not by the inhibitors of nitric oxidase synthase, cyclooxygenase, xanthine oxidase, and the inhibitors of mitochondrial respiratory chain complexes, suggesting that AOPP-triggered podocyte apoptosis is mainly mediated by PKC-NADPH oxidase-dependent O_2^- generation (Figure 3d).

AOPP challenge increased NADPH-dependent O_2^- generation *in vitro* and *in vivo*

To further confirm the presence of oxidative stress and the enzyme source of O_2^- in AOPP-challenged podocytes, oxidase activity in response to the addition of various substrates was examined in podocyte homogenates. As shown in Figure 4a, O_2^- production derived from NADPH was greater than that obtained from other potential substrates. NADPH-dependent O_2^- production was significantly enhanced in AOPP-treated podocytes compared with cells incubated with medium alone or native MSA (Figure 4b). Furthermore, AOPP-triggered O_2^- generation was almost completely blocked by pretreating podocytes with Gö6983, DPI, apocynin, and c-SOD, but not by inhibitors of other potential enzymes, suggesting that AOPP-triggered O_2^- production in cultured podocytes is dependent on the activation of PKC-NADPH oxidase (Figure 4b).

Similarly, O_2^- production in renal cortex homogenates was significantly increased in AOPP-treated rats compared with that in controls, which could be almost completely inhibited by pretreatment of the homogenates with DPI or c-SOD (Figure 4c).

AOPP challenge activated NADPH oxidase *in vitro* and *in vivo*

To further investigate the mechanisms underlying the induction of O_2^- by AOPPs, we examined the effect of AOPPs on the activity of NADPH oxidase. AOPP-MSA induced rapid phosphorylation of the cytoplasmic subunit $p47^{phox}$ in cultured podocytes (Figure 5a). AOPP-induced $p47^{phox}$ phosphorylation could be blocked by pretreatment of podocytes with a PKC inhibitor, Gö6983 (Figure 5a).

To examine the interaction of $p47^{phox}$ with the membrane subunits, we immunoprecipitated $p22^{phox}$, Nox 2, and Nox 4 with the specific antibodies, and then probed for the coexistence of $p47^{phox}$. As shown in Figure 5b, the amount of $p47^{phox}$–$p22^{phox}$ complex formation rapidly increased in AOPP-stimulated podocytes. At 15 min after AOPP challenge, $p47^{phox}$ membrane translocation was apparent (Figure 5c). AOPPs also promoted the association of $p47^{phox}$ with Nox 2 and Nox 4 (Figure 5d).

The increased expression of NADPH oxidase subunits might be necessary for its sustained activation. To examine

Table 2 | AOPP challenge reduced podocyte number and glomerular podocyte density

Parameters	Vehicle (*n*=7)	RSA (*n*=7)	AOPPs (*n*=7)	AOPPs+Apocynin (*n*=7)	*P* value
$N_{podocyte}$	160.2 ± 22.5	160.7 ± 18.4	130.4 ± 21.0[a]	154.4 ± 18.8[b]	<0.05
$V_{glomerulus}$	500,999 ± 99,111	521,552 ± 92,691	627,689 ± 95,392[a]	59,9019 ± 12,2731	<0.05
Nv (Podo/glom)	0.00033 ± 0.00007	0.00032 ± 0.00008	0.00021 ± 0.00003[a]	0.00026 ± 0.00003[b]	<0.05

AOPP, advanced oxidation protein product; $N_{podocyte}$, mean podocyte number/glomerulus; $V_{glomerulus}$, glomerular volume (μm^3); Nv (Podo/glom), numerical density of podocyte/glomerulus; RSA, rat serum albumin.
Data are mean ± s.d.
[a]$P<0.05$ vs vehicle.
[b]$P<0.05$ vs AOPPs.

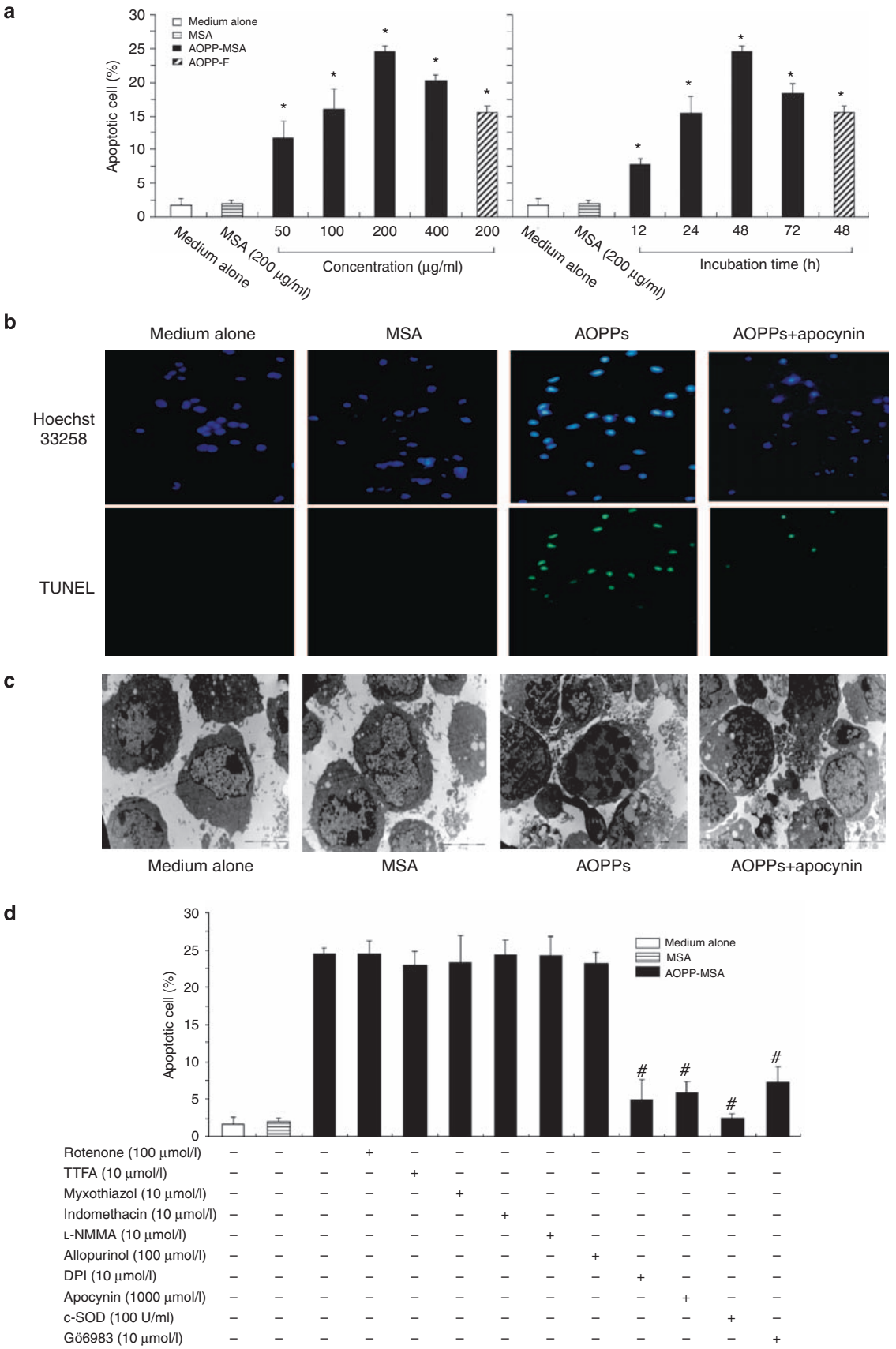
a
Medium alone
MSA
AOPP-MSA
AOPP-F
Apoptotic cell (%)
Medium alone
MSA (200 μg/ml)
50
100
200
400
200
Concentration (μg/ml)
Medium alone
MSA (200 μg/ml)
12
24
48
72
48
Incubation time (h)
b
Medium alone
MSA
AOPPs
AOPPs+apocynin
Hoechst 33258
TUNEL
c
Medium alone
MSA
AOPPs
AOPPs+apocynin
d
Medium alone
MSA
AOPP-MSA
Apoptotic cell (%)
Rotenone (100 μmol/l)
TTFA (10 μmol/l)
Myxothiazol (10 μmol/l)
Indomethacin (10 μmol/l)
L-NMMA (10 μmol/l)
Allopurinol (100 μmol/l)
DPI (10 μmol/l)
Apocynin (1000 μmol/l)
c-SOD (100 U/ml)
Gö6983 (10 μmol/l)

the effect of AOPPs on the expression of the oxidase subunits, podocytes were incubated with AOPP-MSA for 1–12 h. Compared with cells incubated with native MSA, podocytes treated with AOPP-MSA showed significantly increased expression of $p47^{phox}$, Nox 2, and Nox 4, after 3 h of stimulation (Figure 5e). Similarly, renal cortex homogenates from the AOPP-treated rats showed a significantly upregulated expression of $p47^{phox}$ and Nox homologs compared with controls (Figure 5f).

AOPP-induced apoptosis was associated with increased p53 and Bax protein synthesis and caspase-3 activity

Upregulation of p53 has been reported to mediate apoptosis through Bax protein expression in response to a number of stress signals.[2,32] To examine the potential mediators of AOPP-induced apoptosis, we analyzed the abundance of p53 and Bcl-2 family proteins (Bax and Bcl-2) and that of caspase-3 by western blot analysis. AOPP challenge increased p53 expression in cultured podocytes from 2 h. Proapoptotic Bax expression was increased from 6 h (Figure 6a), followed by a decrease in procaspase-3 levels and increase in cleaved caspase-3 at 6–48 h of AOPPs treatment (Figure 6b). Levels of intact 113-kDa PARP (poly (adenosine diphosphate-ribose) polymerase), a substrate of activated caspases, were decreased from 12 h, coincident with the appearance of 85-kDa PARP cleavage products (Figure 6b). These data suggest that AOPP-induced apoptosis is associated with increase activity of the p53-Bax–caspase-3 pathway. Enhanced expression of p53 and Bax protein and activation of caspase-3, could be blocked by the inhibitors of PKC and NADPH oxidase, suggesting that AOPP-induced activation of proapoptotic molecules is mainly mediated by PKC-NADPH oxidase-dependent O_2^- generation (Figure 6c). Consistent with the *in vitro* observation, western blot analysis of the renal cortex homogenates showed upregulation of p53, Bax, and caspase-3 in AOPP-treated rats (Figure 6d).

DISCUSSION

Increased recognition of AOPPs, as a class of potential renal pathogenic mediators and the multiple means by which they form in diverse disorders, has highlighted the importance of determining mechanisms by which AOPPs might induce or promote the progression of glomerulopathy. This study provided *in vivo* and *in vitro* evidence showing that the accumulation of AOPPs triggers podocyte apoptosis and results in podocyte depletion through NADPH oxidase-dependent O_2^- generation. AOPP-albumin, but not native albumin, altered the life span of the podocyte, suggesting that the triggering effect is due to AOPPs and is not a property of albumin or other contaminants. To the best of our knowledge, this is the first study showing the role of AOPPs in the pathogenesis of podocyte depletion.

Podocyte depletion has been proposed as a hallmark of primary and secondary forms of glomerulosclerosis for many years.[6,33] The extent of podocyte depletion is now considered a central problem in the progression of both diabetic and nondiabetic nephropathy.[10,12,34,35] Although clinical and animal studies clearly demonstrate the phenomenon of podocyte depletion in various glomerular diseases, the mechanism(s) underlying podocyte loss have not been completely understood. Podocyte apoptosis has been shown to be a glomerular phenotype that coincides with the onset of albuminuria and is associated with progressive podocyte depletion.[14,15] Several factors have been suggested to induce podocyte apoptosis; hyperglycemia, transforming growth factor-β, and angiotensin II have been extensively characterized.[14–17] In this study, we identified AOPP accumulation as a new candidate mechanism for podocyte apoptosis and podocyte depletion. As we have reported previously,[24,36] chronic administration of AOPP-albumin in normal rats increased the plasma concentration of AOPPs to the level that has been found in diabetic plasma and increased AOPP deposition in the renal tissue. In this model, podocyte apoptosis developed at week 5 and coincided with the onset of albuminuria. The *in vitro* study also showed that both AOPP-MSA and AOPP fraction isolated from uremic patients triggered podocyte apoptosis in a dose- and time-dependent manner. It is noteworthy that, apoptosis of tubular epithelial cells was also increased in AOPP-treated rats, suggesting that epithelial cells might be selectively susceptible to AOPP-induced apoptosis. Interestingly, a recent *in vitro* study has also shown that AOPP challenge promotes renal tubular cells injury through a CD36-dependent pathway.[37] Our very recent finding shows that AOPPs also target mesangial cells,[38] suggesting that at least some of the renal pathogenic effects of AOPPs might be mediated by the mechanism independent of podocyte lesion.

Importantly, this study shows that AOPP-triggered apoptosis is sufficient to induce podocyte loss *in vivo*. The

Figure 3 | AOPPs triggered apoptosis in cultured podocytes by NADPH oxidase-dependent O_2^- generation. (**a**) Podocytes were incubated with AOPP-MSA or AOPP fraction (AOPP-F) isolated from uremic patients for indicated time. Apoptotic podocytes, determined by Annexin V-labeled cells, significantly increased in a dose- and time-dependent manner. $^*P<0.05$ vs medium alone. (**b**) Representative photographs showing TUNEL-positive apoptotic cells in cultured podocytes. Apocynin treatment attenuated AOPP-induced podocyte apoptosis. (**c**) Representative electron micrographs of podocytes incubated with or without AOPP-MSA (original magnification: ×8,000). Treatment with apocynin attenuated AOPP-induced podocyte apoptosis. (**d**) Podocytes were preincubated with the inhibitors of mitochondrial respiratory chain complexes (rotenone; TTFA, and myxothiazol), an inhibitor of nitric oxidase (L-NMMA), a xanthine oxidase inhibitor (allopurinol), the inhibitors of NADPH oxidase (DPI and apocynin), a O_2^- scavenger (c-SOD), and a PKC inhibitor (Gö6983). The cells were then incubated with 200 μg/ml of AOPP-MSA for 48 h. Apoptosis was quantified by measuring Annexin V-labeled cells using a flow cytometer. Data are expressed as mean ± s.d. of three independent experiments. $^{\#}P<0.01$ vs AOPPs. AOPP, advanced oxidation protein product; c-SOD, Cu/Zn superoxide dismutase; DPI, diphenyleneiodonium; MSA, murine serum albumin; NADPH, nicotinamide adenine dinucleotide phosphate; PKC, protein kinase C; TTFA, thenoyltrifluoroacetone; TUNEL, terminal deoxyuridine nick-end labeling.

following lines of evidence support this conclusion. First, podocyte apoptosis coincided with the onset of podocyturia and 68% of urinary podocytes underwent apoptosis. Consistent with this finding, a previous study indicated that podocyturia is associated with podocyte loss and progression of IgA nephropathy, a disorder with the prevalence of AOPP accumulation.[12,26] Second, morphological observation of the AOPP-challenged kidney showed structural changes in response to loss of podocytes and denudation of glomerular basement membrane. Third, reduction in podocyte number and decreased glomerular podocyte density, as judged by the unbiased stereological methods, further confirmed the loss of podocytes in AOPP-treated animals. A progressive depletion of podocytes results in denuded glomerular basement membrane areas and tuft adhesions that has been considered as initial lesions of irreversible glomerular damage.[39] Furthermore, the inability to undergo cell regeneration after podocyte damage may also result in glomerulosclerosis.[40] Taken together, our finding suggests that accumulation of AOPPs might be involved in the initiation or progression of CKD by promoting podocyte depletion. Supporting the notion, our previous studies have shown that chronic accumulation of AOPPs promotes renal damage in a diabetic model and accelerates glomerulosclerosis in the remnant kidney.[12,25]

In this study, we also showed that AOPP-induced podocyte apoptosis and depletion are mainly mediated by NADPH oxidase-dependent superoxide generation. Human and rodent podocytes express the components of NADPH oxidase including $p47^{phox}$, $p22^{phox}$, and Nox homologs. NADPH oxidase represents the major source of superoxide

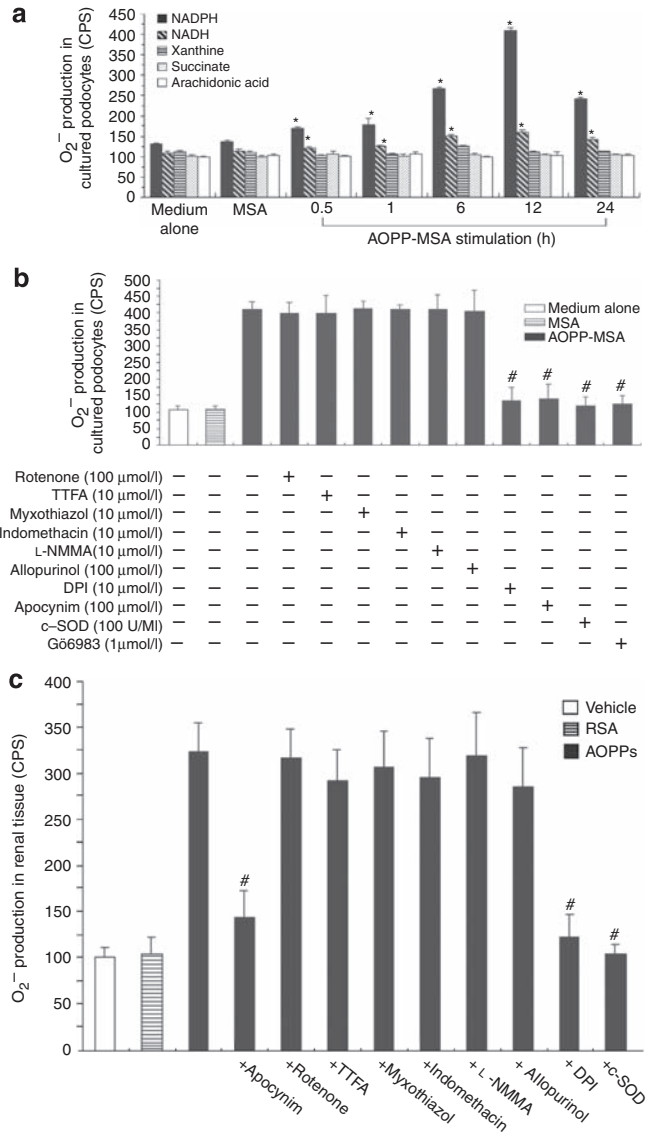

Figure 4 | AOPP challenge increased NADPH-dependent O_2^- production in cultured podocytes and in the renal cortex. (**a**) O_2^- production in response to the addition of various substrates (NADPH, NADH, xanthine, succinate, and arachidonic acid) was determined in podocyte homogenates using the lucigenin chemiluminescence method. (**b**) Podocytes were pretreated with the inhibitors of various enzymes and then incubated with AOPP-MSA. AOPP-triggered O_2^- generation was almost completely blocked by pretreatment with the inhibitors of PKC and NADPH oxidase, as well as c-SOD. (**c**) O_2^- production in the renal cortex, determined by the lucigenin counts, significantly increased in AOPP-treated rats compared with controls. AOPP-induced O_2^- generation was inhibited by pretreatment of renal homogenates with DPI or c-SOD. Data are expressed as mean ± s.d. of three independent experiments. $^*P<0.05$ vs medium alone; $^{\#}P<0.01$ vs AOPPs. AOPP, advanced oxidation protein product; CPS, counts per second; c-SOD, Cu/Zn superoxide dismutase; DPI, diphenyleneiodonium; NADH, nicotinamide adenine dinucleotide; NADPH, nicotinamide adenine dinucleotide phosphate; PKC, protein kinase C.

Figure 5 | AOPP challenge induced activation of NADPH oxidase *in vitro* and *in vivo*. (**a**) Podocytes were incubated with 200 μg/ml of AOPP-MSA or native MSA for indicated time. Phosphorylation of $p47^{phox}$ was assayed by immunoprecipitation (IP) using an α-$p47^{phox}$ and detected by immunoblotting (IB) using an α-pan-$p47^{phox}$ and an α-phosphoserine as the primary antibodies. (**b**) AOPP-induced binding of $p47^{phox}$ to $p22^{phox}$. Podocytes were treated as described above. IP was performed using an α-$p22^{phox}$, and IB was conducted using an α-$p47^{phox}$. (**c**) Representative photographs of AOPP-induced membrane translocation of $p47^{phox}$. Podocytes were incubated with an α-$p47^{phox}$, then with an FITC-conjugated secondary antibody and counterstained with Hoechst 33258 (bar = 30 μm). (**d**) Interaction of $p47^{phox}$ with Nox 2 and Nox 4. Podocytes were treated as described above. IP was performed using an α-Nox 2 or an α-Nox 4. IB was conducted using an α-$p47^{phox}$. (**e**) Expression of NADPH oxidase subunits in cultured podocytes. Podocytes were incubated with or without AOPPs for 1–12 h. Protein expression of NADPH oxidase was determined by western blot using the antibodies against the subunits of NADPH oxidase. (**f**) Expression of NADPH oxidase subunit protein in the renal cortex at week 5 was analyzed as described above. Data are expressed as mean ± s.d. of three independent experiments (*in vitro* experiments) or of five animals per group (*in vivo* experiments). $^*P<0.05$ vs medium alone (*in vitro* experiments) and vehicle (*in vivo* experiments). $^{\#}P<0.05$ vs AOPPs. AOPP, advanced oxidation protein product; FITC, fluorescein isothiocyanate; MSA, murine serum albumin; NADPH, nicotinamide adenine dinucleotide phosphate.

generation in both cultured podocytes and in the renal cortex.[39,41] In this study, we first showed that AOPP challenge induced overproduction of O_2^- in cultured podocytes and in the in renal cortex. AOPP-induced O_2^- production was NADPH dependent and could be blocked by the inhibitors of NADPH oxidase. Next, we examined the activity of NADPH oxidase in AOPP-challenged podocytes. Exposure of podocytes to AOPPs induced rapid phosphorylation of the cytoplasmic subunit $p47^{phox}$ and its membrane translocation; this was followed by increased interaction of $p47^{phox}$ with the

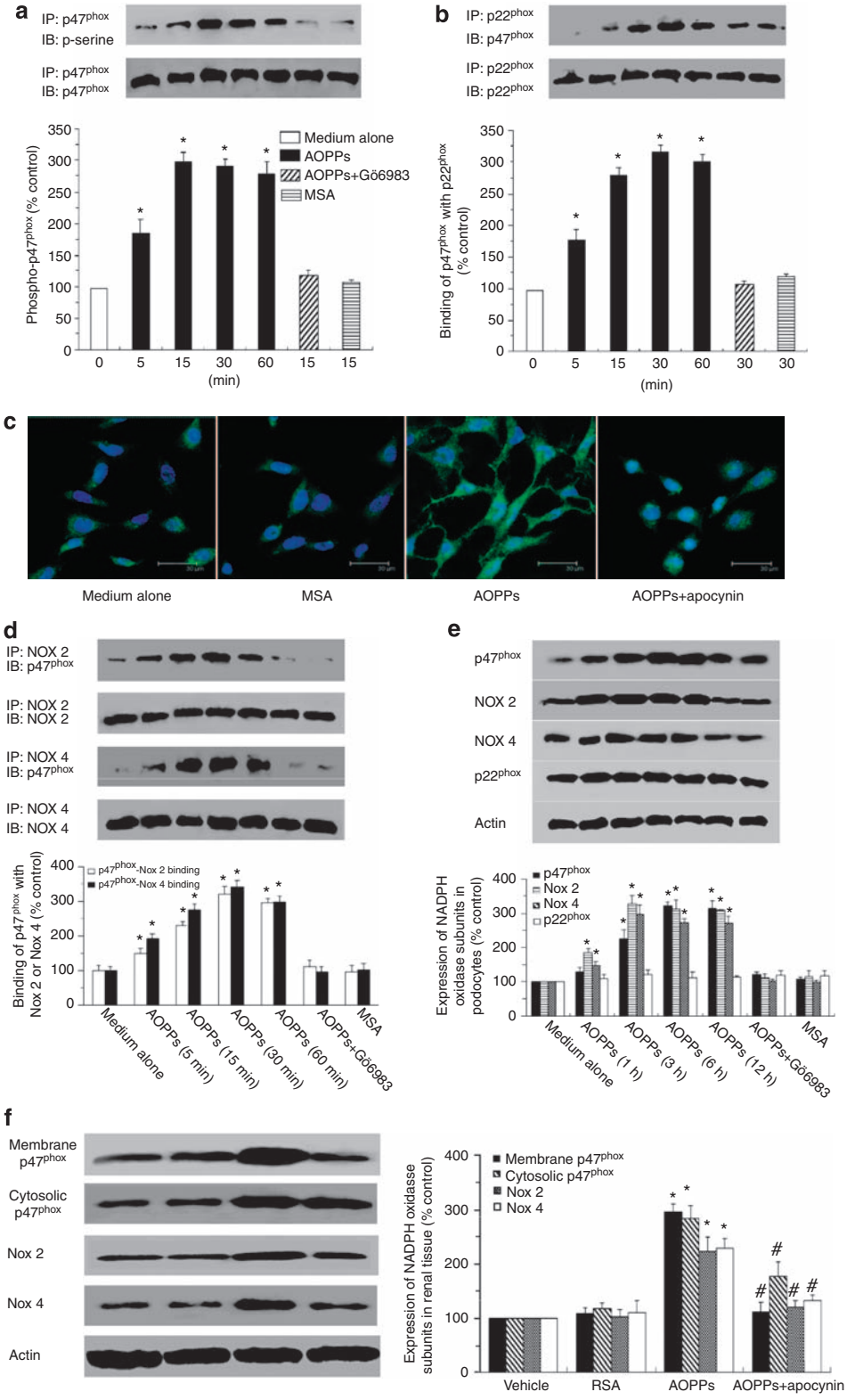

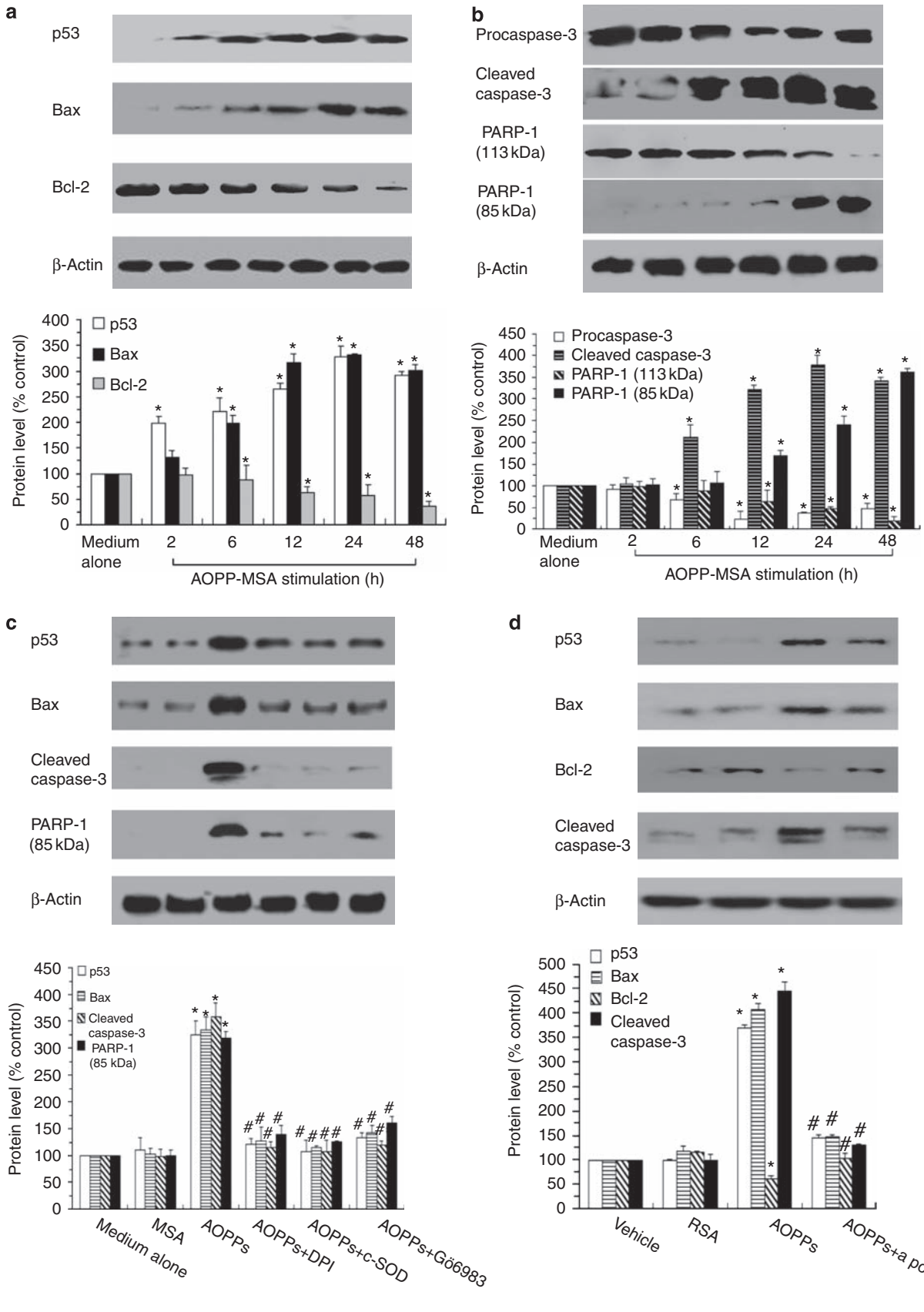
a
p53
Bax
Bcl-2
β-Actin
Protein level (% control)
Medium alone
AOPP-MSA stimulation (h)
b
Procaspase-3
Cleaved caspase-3
PARP-1 (113 kDa)
PARP-1 (85 kDa)
β-Actin
Protein level (% control)
Medium alone
AOPP-MSA stimulation (h)
c
p53
Bax
Cleaved caspase-3
PARP-1 (85 kDa)
β-Actin
Protein level (% control)
Medium alone
MSA
AOPPs
AOPPs+DPI
AOPPs+c-SOD
AOPPs+Gö6983
d
p53
Bax
Bcl-2
Cleaved caspase-3
β-Actin
Protein level (% control)
Vehicle
RSA
AOPPs
AOPPs+a pocynin

membrane subunits $p22^{phox}$, Nox 2, and Nox 4, confirming the activation of total oxidase in AOPP-triggered podocytes. Furthermore, we showed that expression of the key subunits of NADPH oxidase, including that of $p47^{phox}$, $p22^{phox}$, Nox 2, and Nox 4, was upregulated in cultured podocytes after 3 h of exposure to AOPPs. Overexpression of these NADPH oxidase subunits was also found in the renal cortex of rats treated with AOPPs. Finally, we provided data showing that AOPP-induced apoptosis could be largely blocked by pretreating podocytes with the NADPH oxidase inhibitors and the intracellular O_2^- scavenger *in vitro*, or by the intervention of apocynin *in vivo*. Oxidant-dependent DNA damage in podocytes has also been found in puromycin aminonucleoside-treated rats.[18] These data suggest that NADPH oxidase-dependent O_2^- generation constitutes a major pathway resulting in AOPP-induced podocyte apoptosis. This was validated in principle *in vivo* after the chronic inhibition of NADPH oxidase in diabetic models.[25,42,43] The pathophysiological relevance of NADPH oxidase activation in the induction of renal oxidative stress is further supported by the observation of increased urinary 8-OHdG.

Activation of NADPH oxidase occurs through multiple signaling pathways;[44] however, several studies have demonstrated a critical role of PKC.[1,45,46] In this study, a broad spectrum inhibitor of PKC (Gö6983) inhibited AOPP-induced NADPH oxidase activation and O_2^- production, and blocked subsequent apoptosis in cultured podocytes, suggesting that PKC may be located upstream of oxidase activation in the signaling pathway that leads to AOPP-induced O_2^- production.

Both podocyte growth and apoptosis are complexly regulated by the Bcl-2 family, including both proapoptotic molecules (such as Bax) and antiapoptotic molecules (such as Bcl-2). These molecules are regulators of caspases, which serve as the terminal effectors molecules in many types of apoptosis.[47] In this study, we found that AOPP challenge increased p53 accumulation in podocytes. Furthermore, the expression of proapoptotic molecule Bax protein and the activity of effector caspase-3 were significantly increased by treatment with AOPPs. As p53 has been reported to mediate programmed cell death through Bax protein expression in response to a number of stress signals,[2,32] AOPP challenge might induce apoptosis in the podocyte through p53-dependent Bax expression. It is noteworthy that the kinetic profile in this study showed significant induction of O_2^- content as early as 0.5 h; this was followed by the upregulation of p53 after 2 h of exposure and increased expression of Bax after 6 h of incubation. Moreover, the AOPP-triggered p53-Bax-caspase pathway could be almost completely blocked by c-SOD and NADPH oxidase inhibitor, suggesting that the proapoptotic pathway is activated by superoxide produced by NADPH oxidase activation.

In summary, we conclude that accumulation of AOPPs promotes podocyte depletion by the induction of podocyte apoptosis, which is mainly mediated by NADPH oxidase-dependent O_2^- generation. Given that AOPP accumulation is prevalent in diverse pathophysiological conditions such as diabetes, metabolic syndrome, and CKD, this finding might be highly significant because it might be an important step toward understanding the renal pathogenic effects of AOPPs and may provide new targets for the prevention of progressive glomerulosclerosis seen in these disorders.

MATERIALS AND METHODS

AOPP-albumin preparation

AOPP-RSA and AOPP-MSA were prepared *in vitro* by incubation of RSA or MSA (Sigma Chemical, St Louis, MO, USA) with 200 mmol/l of hypochlorous acid (Fluke, Buchs, Switzerland) in the absence of free amino acid/carbohydrates/lipids to exclude the formation of advanced glycation end products–like structures.[19,24] Prepared samples were dialyzed against phosphate-buffered saline to remove free hypochlorous acid. AOPP fraction formed *in vivo* was isolated from the serum of patients with uremia using HiPrep 16/60 Sephacryl S-300HR column (GE Healthcare Bio-Sciences AB, Uppsala, Sweden) as described previously.[48] The concentration of AOPP fraction in patients' serum was $\sim$200 μg/ml.[48] All samples were passed through a DetoxiGel column (Pierce, Rockford, IL, USA) to remove contaminated endotoxin. The endotoxin levels in the preparations were tested using the Amebocyte Lysate Kit (Sigma Chemical) and were found to be <0.025 EU/ml.

AOPP content in the preparation, as determined by the absorbance of the reaction mixture of the samples and acetic acid,[19,24] was 56.4 ± 4.3 nmol/mg protein in AOPP-RSA, 73.6 ± 8.4 nmol/mg protein in AOPP-MSA, 0.30 ± 0.03 nmol/mg protein in native RSA, and 0.25 ± 0.02 nmol/mg protein in native MSA. The components of advanced glycation end products were undetectable in the prepared samples.[49–51]

Cell culture

Murine podocytes were generously provided by Professor Peter Mundel (Sinai School of Medicine, New York, NY, USA) and cultured as described previously.[52] Undifferentiated podocytes were grown in RPMI 1640 containing 10% fetal bovine serum, penicillin (100 U/ml), streptomycin (100 μg/ml), sodium pyruvate (1 mmol/l), HEPES buffer (10 mmol/l), and sodium bicarbonate (0.075%) (all obtained from Sigma Chemical). To passage the cells, podocytes were grown under 'growth-permissive' conditions, which involved growing cells at 33 °C in the presence of interferon-γ (50 U/ml, Sigma Chemical). For

Figure 6 | AOPP challenge increased p53 and Bax protein synthesis and caspase-3 activity. (**a**) The abundance of p53, Bax, and Bcl-2 in podocytes incubated with or without AOPPs was determined by western blot. AOPP challenge increased p53 expression in cultured podocytes from 2 h and Bax protein synthesis from 6 h. (**b**) AOPP challenge decreased procaspase-3 levels and increased cleaved caspase-3 at 6–48 h of exposure. Levels of intact 113-kDa PARP were decreased from 12 h in AOPP-treated podocytes. (**c**) AOPP-induced upregulation in p53, Bax, and activity of caspase-3 could be blocked by pretreatment of podocytes with Gö6983, DPI, and c-SOD. (**d**) Upregulation of p53, Bax, and caspase 3 in the renal cortex homogenates from rats treated with AOPPs. Data are shown as mean ± s.d. of three independent experiments. $^*P<0.05$ vs medium alone; $^{\#}P<0.05$ vs AOPPs. AOPP, advanced oxidation protein product; Bax, p53- and Bcl-2-associated X; c-SOD, Cu/Zn superoxide dismutase; DPI, diphenyleneiodonium; PARP, poly (adenosine diphosphate-ribose) polymerase.

podocytes to acquire a differentiated phenotype, cells were grown under 'restrictive conditions' at 37 °C in the absence of interferon-γ for more than 12 days. Experiments were carried out using passages 10–18, growth-restricted, conditionally immortalized podocytes.

Animal studies

Male Sprague–Dawley rats (initial weight, 180–200 g, Southern Medical University Animal Experiment Center, Guangzhou, China) were housed in a standard environment with free access to water and diet. The rats were randomly assigned to four groups ($n = 10$ in each group) and received daily intravenous injection of vehicle (phosphate-buffered saline, pH 7.4), native RSA (100 mg/kg per day), AOPP-RSA (100 mg/kg per day), and AOPP-RSA (100 mg/kg per day) with intragastric administration of apocynin (Sigma Chemical, 100 mg/kg per day), separately.[50] The dosages of AOPPs and the internal injection were based on our preliminary studies, in which plasma AOPP levels increase approximately onefold of the normal concentration in rats (the level that has been found in patients with diabetes).[24,25]

The rats were killed at the end of weeks 5 and 12. Their kidneys were collected after perfusion with 50 ml of ice-cold normal saline. AOPP levels in the plasma and renal cortex homogenate were measured as described above.

Assessment of podocyte apoptosis

AV-labeled cells in cultured podocytes. Determination of AV-labeled apoptotic cells was performed as described previously.[53] Cell suspension was incubated with either fluorescein isothiocyanate (FITC)-conjugated AV alone, propidium iodide (PI) alone, or a combination of both according to the manufacturer's instructions (KeyGen, Nanking, China). Cells were analyzed using a flow cytometer (BD FACSCalibur System, Franklin Lakes, NJ, USA), with excitation at 488 nm and emission at 525 nm (for AV-labeled cells) and 620 nm (for PI-labeled cells). Single labeling was used to gate and control for bleed through. Cell population was characterized on the basis of whether it was labeled with neither AV nor PI (viable), AV alone (apoptotic), PI alone (necrotic), or both AV and PI (late apoptotic).

TUNEL assay in cultured podocytes. DNA strand breaks in cultured podocytes were identified using TUNEL as described previously.[49] The cells were fixed in 4% paraformaldehydrate followed by methanol. After washing, cells were incubated in TDT buffer containing the TdT enzyme and FITC-conjugated dUTP according to the manufacturer's protocol (KeyGen). Morphological changes in cells undergoing apoptosis were detected simultaneously by counterstaining them with Hoechst 33258 (KeyGen, Nanking, China). The slides were examined by fluorescent microscopy (Leica TCS SP2 AOBS, Leica Microsystems, Cambridge, UK).

Analysis of podocyte apoptosis in renal tissue. Apoptotic cells were detected on frozen kidney section using FITC-labeled *in situ* Apoptosis Detection Kit (KeyGen, Wuhan, China). For identification of the apoptotic podocyte, tissue sections were costained with anti-Wilms's tumor-1 antibody (red) and TUNEL (green). The cells double labeled by Wilms's tumor-1 and TUNEL were counted as apoptotic podocytes.

Identification of apoptotic podocytes in urine. Rat sterile urine was collected by bladder puncture as described previously.[54] Resuspended cell pellets were centrifuged onto polylysine-coated slides, fixed with 3% paraformaldehyde, and then permeabilized with Triton X-100. After blocking with 1% bovine serum albumin, the slides were incubated with a goat anti-rat podocalyxin antibody (Santa Cruz Biotechnology, Santa Cruz, CA, USA) and then with the secondary antibody TRITC-labeled donkey anti-goat IgG (Santa Cruz Biotechnology). The sediments were counterstained with Hoechst nuclear stain to distinguish whole cells from cell fragments. TUNEL staining for apoptosis was performed on the specimens using a standard FITC incorporation kit (KeyGen) according to the package instructions. The slides were examined using a fluorescence microscope (BX51, Olympus, Tokyo, Japan) at 590 nm for podocalyxin, 488 nm for TUNEL, and 460 nm for Hoechst. Nucleated, podocalyxin-positive cells were considered to be detached podocytes and those with a positive staining of FITC were regarded as apoptotic podocytes. Urinary podocyte number was quantified in a blinded manner and was shown as cells per milliliter urine.

Expression of apoptosis-related molecules. To measure the protein expression of apoptosis-related molecules, cultured cells were lysed and the frozen renal cortex was processed for protein extraction as described previously.[55] The protein samples were subjected to 8–12% SDS-PAGE before being transferred into PVDF (polyvinylidene fluoride) membranes (NEN Life Science Products, Boston, MA, USA). Western blotting was performed as described elsewhere[56] using the following primary antibodies: anti-p53 mAb (Oncogene Research Products, San Diego, CA, USA), anti-Bax mAb (Santa Cruz Biotechnology), polyclonal rabbit anti-caspase-3 (Cell Signaling Technology, Beverly, MA, USA), anti-Bcl-2 mAb (Santa Cruz Biotechnology), and anti-PARP mAb (Cell Signaling Technology). Bound primary antibodies were detected with horseradish peroxidase (HRP)-labeled anti-mouse or anti-rabbit secondary antibodies, and visualized using enhanced chemiluminescence reagents (Pierce Chemical, Bockford, IN, USA).

Morphological observation

Renal cortex or podocyte sediment was processed through a primary and a secondary fixation, acetone dehydration, and then Epon-Spurr's resin infiltration as described previously.[57] Samples were rocked overnight and then embedded and polymerized at 60 °C for 24 h. Thin sections (80 nm) were collected and stained with uranyl acetate and lead citrate. A transmission electron microscope (Hitachi, Tokyo, Japan) was used to observe the samples.

Immunohistochemical analysis of ki-67 and PCNA

The expression of ki-67 and PCNA in the kidney section was determined as described previously.[58,59] The sections of paraffin-embedded tissues were rehydrated in phosphate-buffered saline and subjected to microwave heating. The sections were stained by monoclonal anti-ki-67 antibody (Dako, Carpinteria, CA, USA) or monoclonal mouse anti-rat PCNA antibody (Boster, Wuhan, China) and then detected using the Vectastain Elite ABC Kit (Vector Laboratories, Burlingame, CA, USA).

Determination of podocyte number and density in the glomerulus

Sections of 1-μm thickness from the Spurrs blocks were used for the studies. After facing the block, the first intact section was saved and numbered 0. At least 200 serial sections were then cut from each kidney. Every 19th and 20th section was saved together on a slide so that at least 10 pairs of sections were available for analysis from each rat. All sections were stained with 1% toluidine blue. The first five glomeruli not present in section 0, but appearing and disappearing in subsequent sections, were mapped to a location within the sections and were numbered 1–5. An Olympus BX51 microscope, fitted with a digital camera and DP Controller software (Olympus, Tokyo, Japan)

was used to obtain images of the all sections containing glomeruli 1–5. The $\times 100$ oil lens was used giving a final image magnification of 1680. Adobe Photoshop version CS3 (Adobe Systems Incorporated, San Jose, CA, USA) was used to observe images.

The number of podocyte ($N_{podocyte}$) was counted using the Disector/Fractionator technique as described previously.[60–62] Glomerular volume ($V_{glomerulus}$) was measured using the Cavalieri principle as described elsewhere.[61–63] The numerical density of podocyte per glomerulus (Nv (Podo/glom)) was calculated using the equation, $Nv\ (Podo/glom) = N_{podocyte}/V_{glomerulus}$.

Estimation of NADPH oxidase activity

NADPH-dependent O_2^- production. NADPH-dependent O_2^- production by homogenates from cultured podocytes or the renal cortex was assessed by lucigenin-enhanced chemiluminescence as described previously.[64] The chemiluminescence value was recorded every minute for 30 min (Victor V Wallac 1420, Perkin-Elmer, Turku, Finland). The readings in each of the last 5 min were averaged and expressed as counts per second.

P47^{phox} phosphorylation. Phosphorylation of P47^{phox} in cultured podocytes was detected by immunoprecipitation as described previously.[65] Briefly, the cell lysates were preabsorbed with protein A/G agarose beads (Santa Cruz Biotechnology) and incubated with a polyclonal rabbit anti-p47^{phox} antibody (Santa Cruz Biotechnology). The immunocomplexes were resolved with SDS-PAGE, transferred into nitrocellulose membranes (Amersham Pharmacia Biotech, Piscataway, NJ, USA), and incubated with a HRP-conjugated rabbit anti-phosphoserine antibody (Stressgen Bioreagents, Victoria, BC, Canada). The blots were detected with ECL (Pierce). To determine pan-p47^{phox}, the membranes were washed with an elute buffer, reacted with an anti-p47^{phox} mAb (BD Biosciences Pharmingen, San Diego, CA, USA), and subsequently detected with HRP-conjugated rabbit anti-mouse IgG (DakoCytomation, Glostrup, Denmark) and ECL. Bands were quantified by densitometry (Universal Hood. 2, BioRad, Milan, Italy), and values were normalized to the amount of total p47^{phox} per sample.

Interaction of p47^{phox} with p22^{phox} and Nox homologs. The interaction of p47^{phox} with p22^{phox} and Nox homologs in cultured podocytes was analyzed by immunoblotting as described previously.[66] The immunocomplexes were obtained by incubation of cell lysates with a rabbit anti-mouse p22^{phox}, a goat anti-mouse Nox 2, or a rabbit anti-mouse Nox 4 antibody (all from Santa Cruz Biotechnology), separately. Immunoblotting was performed using the rabbit anti-mouse p47^{phox} antibody (Santa Cruz Biotechnology) as the primary antibody and the HRP-conjugated swine anti-rabbit IgG (DakoCytomation) as the secondary antibody. The membranes were detected by ECL. To determine the total p22^{phox}, Nox 2, or Nox 4, the membranes were eluted and incubated with the anti-mouse p22^{phox}, Nox 2, or Nox 4 antibodies and then detected with the HRP-conjugated anti-rabbit or goat IgG antibody (DakoCytomation).

P47^{phox} membrane translocation. Cultured podocytes were fixed in acetone–methanol (1:1, vol/vol). After washing and blocking, the cells were incubated overnight with a rabbit anti-mouse p47^{phox} antibody at 4 °C. After washing, the slides were incubated with a FITC-conjugated swine anti-rabbit IgG (DakoCytomation) antibody for 45 min at 37 °C, washed, stained with Hoechst (KeyGen) and observed under a confocal microscopy (Leica TCS SP2 AOBS, Leica Microsystems).

Expression of NADPH oxidase subunits. Membrane proteins were extracted using a ProteoExtract kit (Calbiochem, San Diego, CA, USA) according to the manufacturer's instructions. Expression of NADPH oxidase subunits in the membrane and cytosolic fraction was analyzed by western blot as described elsewhere.[67] The primary antibody was a rabbit anti-p47^{phox}, a rabbit anti-p22^{phox}, a goat anti-Nox 2, or a rabbit anti-Nox 4 antibodies (all from Santa Cruz Biotechnology). The secondary antibody was a HRP-conjugated anti-rabbit or anti-goat IgG antibody.

Statistical analysis

All experiments were carried out in triplicate. Continuous variables, expressed as mean ± s.d., were compared using one-way ANOVA (analysis of variance). Pairwise comparisons were evaluated by the Student–Newman–Keuls procedure or Dunnett's T3 procedure when the assumption of equal variances did not hold. The Dunnett procedure was used for comparisons between reference group and other groups. A two-tailed P-value of <0.05 was considered statistically significant. Statistical analyses were conducted using SPSS 13.0 (SPSS Inc., Chicago, USA).

DISCLOSURE

All the authors declared no competing interests.

ACKNOWLEDGMENTS

We thank Peter Mundel for providing murine podocytes and John Basgen (Department of Pediatrics, University of Minnesota Medical Center, Minneapolis, MN, USA) for his assistance on stereological analyses. This study was supported by a National Nature and Science Grant (No. 30830056) and a National 973 program grant (No. 2006CB503904) to FFH.

REFERENCES

1. Kitada M, Koya D, Sugimoto T *et al.* Translocation of glomerular p47phox and p67phox by protein kinase C-beta activation is required for oxidative stress in diabetic nephropathy. *Diabetes* 2003; **52**: 2603–2614.
2. Choudhuri T, Pal S, Agwarwal ML *et al.* Curcumin induces apoptosis in human breast cancer cells through p53-dependent Bax induction. *FEBS Lett* 2002; **512**: 334–340.
3. Eddy AA. Molecular insights into renal interstitial fibrosis. *J Am Soc Nephrol* 1996; **7**: 2495–2508.
4. Remuzzi G, Ruggenenti P, Perico N. Chronic renal diseases: renoprotective benefits of renin-angiotensin system inhibition. *Ann Intern Med* 2002; **136**: 604–615.
5. Pavenstadt H, Kriz W, Kretzler M. Cell biology of the glomerular podocyte. *Physiol Rev* 2003; **83**: 253–307.
6. Kriz W, Gretz N, Lemley KV. Progression of glomerular diseases: is the podocyte the culprit? *Kidney Int* 1998; **54**: 687–697.
7. Wolf G, Chen S, Ziyadeh FN. From the periphery of the glomerular capillary wall toward the center of disease: podocyte injury comes of age in diabetic nephropathy. *Diabetes* 2005; **54**: 1626–1634.
8. Toyoda M, Najafian B, Kim Y *et al.* Podocyte detachment and reduced glomerular capillary endothelial fenestration in human type 1 diabetic nephropathy. *Diabetes* 2007; **56**: 2155–2160.
9. White KE, Bilous RW. Structural alterations to the podocyte are related to proteinuria in type 2 diabetic patients. *Nephrol Dial Transplant* 2004; **19**: 1437–1440.
10. Pagtalunan ME, Miller PL, Jumping-Eagle S *et al.* Podocyte loss and progressive glomerular injury in type II diabetes. *J Clin Invest* 1997; **99**: 342–348.
11. Steffes MW, Schmidt D, McCrery R *et al.* Glomerular cell number in normal subjects and in type 1 diabetic patients. *Kidney Int* 2001; **59**: 2104–2113.
12. Lemley KV, Lafayette RA, Safai M *et al.* Podocytopenia and disease severity in IgA nephropathy. *Kidney Int* 2002; **61**: 1475–1485.
13. Lemley KV, Lafayette RA, Derby G *et al.* Prediction of early progression in recently diagnosed IgA nephropathy. *Nephrol Dial Transplant* 2008; **23**: 213–222.
14. Schiffer M, Bitzer M, Roberts IS *et al.* Apoptosis in podocytes induced by TGF-beta and Smad7. *J Clin Invest* 2001; **108**: 807–816.

15. Schiffer M, Mundel P, Shaw AS *et al.* A novel role for the adaptor molecule CD2-associated protein in transforming growth factor-beta-induced apoptosis. *J Biol Chem* 2004; **279**: 37004–37012.
16. Susztak K, Raff AC, Schiffer M *et al.* Glucose-induced reactive oxygen species cause apoptosis of podocytes and podocyte depletion at the onset of diabetic nephropathy. *Diabetes* 2006; **55**: 225–233.
17. Ding G, Reddy K, Kapasi AA *et al.* Angiotensin II induces apoptosis in rat glomerular epithelial cells. *Am J Physiol Renal Physiol* 2002; **283**: F173–F180.
18. Marshall CB, Pippin JW, Krofft RD *et al.* Puromycin aminonucleoside induces oxidant-dependent DNA damage in podocytes in vitro and in vivo. *Kidney Int* 2006; **70**: 1962–1973.
19. Witko-Sarsat V, Friedlander M, Capeillere-Blandin C *et al.* Advanced oxidation protein products as a novel marker of oxidative stress in uremia. *Kidney Int* 1996; **49**: 1304–1313.
20. Witko-Sarsat V, Friedlander M, Nguyen KT *et al.* Advanced oxidation protein products as novel mediators of inflammation and monocyte activation in chronic renal failure. *J Immunol* 1998; **161**: 2524–2532.
21. Kalousova M, Skrha J, Zima T. Advanced glycation end-products and advanced oxidation protein products in patients with diabetes mellitus. *Physiol Res* 2002; **51**: 597–604.
22. Martin-Gallan P, Carrascosa A, Gussinye M *et al.* Biomarkers of diabetes-associated oxidative stress and antioxidant status in young diabetic patients with or without subclinical complications. *Free Radic Biol Med* 2003; **34**: 1563–1574.
23. Atabek ME, Keskin M, Yazici C *et al.* Protein oxidation in obesity and insulin resistance. *Eur J Pediatr* 2006; **165**: 753–756.
24. Li HY, Hou FF, Zhang X *et al.* Advanced oxidation protein products accelerate renal fibrosis in a remnant kidney model. *J Am Soc Nephrol* 2007; **18**: 528–538.
25. Shi XY, Hou FF, Niu HX *et al.* Advanced oxidation protein products promote inflammation in diabetic kidney through activation of renal nicotinamide adenine dinucleotide phosphate oxidase. *Endocrinology* 2008; **149**: 1829–1839.
26. Descamps-Latscha B, Witko-Sarsat V, Nguyen-Khoa T *et al.* Early prediction of IgA nephropathy progression: proteinuria and AOPP are strong prognostic markers. *Kidney Int* 2004; **66**: 1606–1612.
27. Sugiyama H, Kashihara N, Makino H *et al.* Apoptosis in glomerular sclerosis. *Kidney Int* 1996; **49**: 103–111.
28. Hattori T, Shindo S, Kawamura H. Apoptosis and expression of Bax protein and Fas antigen in glomeruli of a remnant-kidney model. *Nephron* 1998; **79**: 186–191.
29. Zhang W, Khanna P, Chan LL *et al.* Diabetes-induced apoptosis in rat kidney. *Biochem Mol Med* 1997; **61**: 58–62.
30. Ying WZ, Wang PX, Sanders PW. Induction of apoptosis during development of hypertensive nephrosclerosis. *Kidney Int* 2000; **58**: 2007–2017.
31. Hoffmann S, Podlich D, Hahnel B *et al.* Angiotensin II type 1 receptor overexpression in podocytes induces glomerulosclerosis in transgenic rats. *J Am Soc Nephrol* 2004; **15**: 1475–1487.
32. Agarwal ML, Taylor WR, Chernov MV *et al.* The p53 network. *J Biol Chem* 1998; **273**: 1–4.
33. Fries JW, Sandstrom DJ, Meyer TW *et al.* Glomerular hypertrophy and epithelial cell injury modulate progressive glomerulosclerosis in the rat. *Lab Invest* 1989; **60**: 205–218.
34. Meyer TW, Bennett PH, Nelson RG. Podocyte number predicts long-term urinary albumin excretion in Pima Indians with type II diabetes and microalbuminuria. *Diabetologia* 1999; **42**: 1341–1344.
35. Dalla VM, Masiero A, Roiter AM *et al.* Is podocyte injury relevant in diabetic nephropathy? Studies in patients with type 2 diabetes. *Diabetes* 2003; **52**: 1031–1035.
36. Liu SX, Hou FF, Guo ZJ *et al.* Advanced oxidation protein products accelerate atherosclerosis through promoting oxidative stress and inflammation. *Arterioscler Thromb Vasc Biol* 2006; **26**: 1156–1162.
37. Iwao Y, Nakajou K, Nagai R *et al.* CD36 is one of important receptors promoting renal tubular injury by advanced oxidation protein products. *Am J Physiol Renal Physiol* 2008; **295**: F1871–F1880.
38. Wei XF, Zhou QG, Hou FF *et al.* Advanced oxidation protein products induce mesangial cell perturbation through PKC-dependent activation of NADPH oxidase. *Am J Physiol Renal Physiol* 2009; **296**: F427–F437.
39. Gill PS, Wilcox CS. NADPH oxidases in the kidney. *Antioxid Redox Signal* 2006; **8**: 1597–1607.
40. Nagata M, Shibata S, Shigeta M *et al.* Cyclin-dependent kinase inhibitors: p27kip1 and p57kip2 expression during human podocyte differentiation. *Nephrol Dial Transplant* 1999; **14**(Suppl 1): 48–51.
41. Greiber S, Munzel T, Kastner S *et al.* NAD(P)H oxidase activity in cultured human podocytes: effects of adenosine triphosphate. *Kidney Int* 1998; **53**: 654–663.
42. Asaba K, Tojo A, Onozato ML *et al.* Effects of NADPH oxidase inhibitor in diabetic nephropathy. *Kidney Int* 2005; **67**: 1890–1898.
43. Thallas-Bonke V, Thorpe SR, Coughlan MT *et al.* Inhibition of NADPH oxidase prevents advanced glycation end product-mediated damage in diabetic nephropathy through a protein kinase C-alpha-dependent pathway. *Diabetes* 2008; **57**: 460–469.
44. Brandes RP, Kreuzer J. Vascular NADPH oxidases: molecular mechanisms of activation. *Cardiovasc Res* 2005; **65**: 16–27.
45. Zhang M, Kho AL, Anilkumar N *et al.* Glycated proteins stimulate reactive oxygen species production in cardiac myocytes: involvement of Nox2 (gp91phox)-containing NADPH oxidase. *Circulation* 2006; **113**: 1235–1243.
46. Frey RS, Rahman A, Kefer JC *et al.* PKCzeta regulates TNF-alpha-induced activation of NADPH oxidase in endothelial cells. *Circ Res* 2002; **90**: 1012–1019.
47. Kanjanabuch T, Ma LJ, Chen J *et al.* PPAR-gamma agonist protects podocytes from injury. *Kidney Int* 2007; **71**: 1232–1239.
48. Guo ZJ, Niu HX, Hou FF *et al.* Advanced oxidation protein products activate vascular endothelial cells via a RAGE-mediated signaling pathway. *Antioxid Redox Signal* 2008; **10**: 1699–1712.
49. Hou FF, Miyata T, Boyce J *et al.* Beta(2)-microglobulin modified with advanced glycation end products delays monocyte apoptosis. *Kidney Int* 2001; **59**: 990–1002.
50. Nagai R, Hayashi CM, Xia L *et al.* Identification in human atherosclerotic lesions of GA-pyridine, a novel structure derived from glycolaldehyde-modified proteins. *J Biol Chem* 2002; **277**: 48905–48912.
51. Sady C, Jiang CL, Chellan P *et al.* Maillard reactions by alpha-oxoaldehydes: detection of glyoxal-modified proteins. *Biochim Biophys Acta* 2000; **1481**: 255–264.
52. Mundel P, Reiser J, Zuniga Mejia BA *et al.* Rearrangements of the cytoskeleton and cell contacts induce process formation during differentiation of conditionally immortalized mouse podocyte cell lines. *Exp Cell Res* 1997; **236**: 248–258.
53. Foster RR, Saleem MA, Mathieson PW *et al.* Vascular endothelial growth factor and nephrin interact and reduce apoptosis in human podocytes. *Am J Physiol Renal Physiol* 2005; **288**: F48–F57.
54. Yu D, Petermann A, Kunter U *et al.* Urinary podocyte loss is a more specific marker of ongoing glomerular damage than proteinuria. *J Am Soc Nephrol* 2005; **16**: 1733–1741.
55. Shihab FS, Andoh TF, Tanner AM *et al.* Expression of apoptosis regulatory genes in chronic cyclosporine nephrotoxicity favors apoptosis. *Kidney Int* 1999; **56**: 2147–2159.
56. Bitzer M, von GG, Liang D *et al.* A mechanism of suppression of TGF-beta/SMAD signaling by NF-kappa B/RelA. *Genes Dev* 2000; **14**: 187–197.
57. Whaley-Connell AT, Chowdhury NA, Hayden MR *et al.* Oxidative stress and glomerular filtration barrier injury: role of the renin-angiotensin system in the Ren2 transgenic rat. *Am J Physiol Renal Physiol* 2006; **291**: F1308–F1314.
58. Moeller MJ, Soofi A, Hartmann I *et al.* Podocytes populate cellular crescents in a murine model of inflammatory glomerulonephritis. *J Am Soc Nephrol* 2004; **15**: 61–67.
59. Ma LJ, Marcantoni C, Linton MF *et al.* Peroxisome proliferator-activated receptor-gamma agonist troglitazone protects against nondiabetic glomerulosclerosis in rats. *Kidney Int* 2001; **59**: 1899–1910.
60. Sterio DC. The unbiased estimation of number and sizes of arbitrary particles using the disector. *J Microsc* 1984; **134**: 127–136.
61. Bertram JF. Analyzing renal glomeruli with the new stereology. *Int Rev Cytol* 1995; **161**: 111–172.
62. Nyengaard JR. Stereologic methods and their application in kidney research. *J Am Soc Nephrol* 1999; **10**: 1100–1123.
63. Gundersen HJ, Jensen EB. The efficiency of systematic sampling in stereology and its prediction. *J Microsc* 1987; **147**: 229–263.
64. Li JM, Mullen AM, Yun S *et al.* Essential role of the NADPH oxidase subunit p47(phox) in endothelial cell superoxide production in response to phorbol ester and tumor necrosis factor-alpha. *Circ Res* 2002; **90**: 143–150.
65. Wolf G, Neilson EG. Angiotensin II as a renal growth factor. *J Am Soc Nephrol* 1993; **3**: 1531–1540.
66. Ziyadeh FN. Mediators of diabetic renal disease: the case for tgf-beta as the major mediator. *J Am Soc Nephrol* 2004; **15**(Suppl 1): S55–S57.
67. Vaziri ND. Roles of oxidative stress and antioxidant therapy in chronic kidney disease and hypertension. *Curr Opin Nephrol Hypertens* 2004; **13**: 93–99.